BIOSCIENCE, BIOTECHNOLOGY, AND BIOCHEMISTRY
2018, VOL. 82, NO. 7, 1143–1152
https://doi.org/10.1080/09168451.2018.1447358

A comparative study of the biomass properties of *Erianthus* and sugarcane: lignocellulose structure, alkaline delignification rate, and enzymatic saccharification efficiency

Takuji Miyamoto[a], Masaomi Yamamura[a], Yuki Tobimatsu[a], Shiro Suzuki[a], Miho Kojima[b#], Keiji Takabe[b], Yoshifumi Terajima[c], Asako Mihashi[d], Yoshinori Kobayashi[d] and Toshiaki Umezawa[a,e]

[a]Research Institute for Sustainable Humanosphere, Kyoto University, Uji, Kyoto, Japan; [b]Graduate School of Agriculture, Kyoto University, Kyoto, Japan; [c]Tropical Agricultural Research Front, Japan International Research Center for Agricultural Sciences, Ishigaki, Japan; [d]Tsukuba Laboratory, AIST Tsukuba Central 6, Japan Bioindustry Association, Tsukuba, Japan; [e]Research Unit for Development of Global Sustainability, Kyoto University, Uji, Kyoto, Japan

ABSTRACT

A comprehensive understanding of the structure and properties of gramineous lignocelluloses is needed to facilitate their uses in biorefinery. In this study, lignocelluloses from fractionated internode tissues of two taxonomically close species, *Erianthus arundinaceus* and sugarcane (*Saccharum* spp.), were characterized. Our analyses determined that syringyl (S) lignins were predominant over guaiacyl (G) or *p*-hydroxyphenyl (H) lignins in sugarcane tissues; on the other hand, S lignin levels were similar to those of G lignin in *Erianthus* tissues. In addition, tricin units were detected in sugarcane tissues, but not in *Erianthus* tissues. Distributions of lignin inter-monomeric linkage types were also different in *Erianthus* and sugarcane tissues. Alkaline treatment removed lignins from sugarcane tissues more efficiently than *Erianthus* tissues, resulting in a higher enzymatic digestibility of sugarcane tissues compared with *Erianthus* tissues. Our data indicate that *Erianthus* biomass displayed resistance to alkaline delignification and enzymatic digestion.

ARTICLE HISTORY
Received 18 January 2018
Accepted 21 February 2018

KEYWORDS
Erianthus; sugarcane; lignocellulose; alkaline treatment; enzymatic saccharification

Lignocellulosic biomass, the most abundant renewable resource on Earth, has long been utilized as a fuel, woody material, and paper feedstock [1]. Recently, lignocellulosic biomass has attracted much attention as a potential feedstock for production of energy and materials in biorefinery. Large gramineous plants such as *Erianthus* spp., sugarcanes (*Saccharum* spp.), *Miscanthus* spp., and Napier grass (*Pennisetum purpureum*) are a potential source of materials with high biomass productivity [2,3]. In particular, *Erianthus* shows 40–60 ton ha^{-1} of dry matter yield [4] and high tolerance to drought, acidity, and infertility [5,6]. In addition, large quantities of nutritional minerals that accumulate in harvestable aerial parts of *Erianthus* are translocated to stubble and root during harvesting [7,8], which is a beneficial for reducing fertilizer input. *Erianthus* is a close relative of sugarcane, which is an important crop for sugar production, and is of interest to sugarcane growers as a genetic resource [9]. Sugarcane could also serve as a feedstock for biorefinery, and therefore, lignocellulose characteristics of sugarcane have been actively studied [10–12]. In contrast, however, earlier reports on characteristics of *Erianthus* lignocellulose are still fewer than those on sugarcane lignocellulose.

Lignocellulose is mainly composed of lignins and polysaccharides (cellulose and hemicelluloses). Enzymatic conversions of cellulose and hemicelluloses to fermentable sugars have been studied extensively in the context of biorefinery. Lignins generally limit the enzymatic saccharification process by impeding the access of hydrolytic enzymes to polysaccharide substrates, and also by deactivating the enzymes through non-selective adsorption [13,14]. Earlier studies have shown that enzymatic saccharification efficiency is negatively correlated with lignin content in numerous plant species, including several large gramineous species [11,15]. However, we previously observed that the saccharification efficiency of *Erianthus* tissues was not always correlated with the lignin content [16], suggesting that some other factors besides lignin content, such as lignin chemical structures [17], xylan presence [18], and conformation of cellulose microfibrils [19], might affect the saccharification of *Erianthus*.

CONTACT Toshiaki Umezawa tumezawa@rish.kyoto-u.ac.jp
[#]Present address: Wood Anatomical and Quality Laboratory, Department of Wood Properties and Processing, Forestry and Forest Products Research Institute, Tsukuba, Ibaraki 305-8687, Japan.

The supplemental data for this article can be accessed at https://doi.org/10.1080/09168451.2018.1447358

Before enzymatic digestion, lignocellulosic biomass is generally pretreated to improve its saccharification efficiency. Alkaline treatment using aqueous NaOH is known to be an effective method for delignification of gramineous biomass [20–24], and hence alkaline delignification efficiency is an important indicator of lignocellulosic biomass utility for fermentable sugar production. Previous studies have suggested that alkaline delignification efficiency could be affected by lignin chemical structure. For example, syringyl (S) units in lignins are preferentially solubilized over guaiacyl (G) units in alkaline pretreatments of sugarcane [12], bamboo (*Bambusa rigida*) [25], and sorghum [26], suggesting that S lignin-abundant biomass will be useful for fermentable sugar production [27]. Thus, an analysis of lignin chemical structures will be important for evaluating a biomass recalcitrance to alkaline delignification.

In this study, to gain insight into the structure and properties of gramineous biomass, we investigated (1) original lignocellulose composition and lignin chemical structures, (2) changes in the lignocellulose composition and lignin chemical structures by an alkaline treatment, and (3) enzymatic saccharification efficiency of fractionated internode tissues from *Erianthus arundinaceus*, and also sugarcane as a control for comparison. To analyze the lignocellulose structures from *Erianthus* and sugarcane tissues before and after the alkaline treatment in details, we used a series of chemical degradation and two-dimensional (2D) nuclear magnetic resonance (NMR) spectroscopy methods. Our data will increase an understanding of biomass from *Erianthus* and sugarcane, which could facilitate their applications to biorefinery.

Materials and methods

Plant materials

Erianthus plants (*E. arundinaceus*, Type I) [28] used in this study were obtained from the Kamigamo Experimental Station, Field Science Education and Research Center, Kyoto University, Japan. Sugarcane (*Saccharum officinarum* cv. NCo310) used for the histochemical analysis was obtained from the Tropical Agriculture Research Front, Japan International Research Center for Agricultural Science, Okinawa, Japan. Sugarcane (*Saccharum* sp.) used for all the other analyses was obtained from a cultivation field in Okinawa, Japan.

Histochemical analysis

Histochemical staining using phloroglucinol-HCl was carried out as described previously [16] using 70-μm-thick and 50-μm-thick tissue sections of internode tissues of *Erianthus* and *S. officinarum*, respectively. The stained sections were imaged under an Olympus BX51 microscope (Olympus Co., Tokyo, Japan) equipped with an Olympus DP71 digital camera (Olympus).

Preparation of cell wall samples

The bottom internodes were divided into inner and outer parts, and then pulverized and extracted with solvents as described previously [16]. Briefly, we fractionated and chopped the inner and outer parts of internode tissues from *Erianthus* and sugarcane with a cork borer and scissors, and pulverized them with a TissueLyser (Qiagen KK, Tokyo, Japan). For sugarcane, chopped samples before pulverization were extracted with methanol (ten times) and water (five times) at 60 °C to remove sugar juice, and freeze-dried. The pulverizations of internode tissues from both *Erianthus* and sugarcane were conducted under a same condition (3 min at 25 Hz at room temperature). The pulverized samples of both species were further extracted with methanol (twenty times), hexane (five times), and water (six times) at 60 °C, room temperature, and 60 °C, respectively. The resulting powder samples were freeze-dried. The obtained powders are referred to as cell wall residue (CWR).

Lignin content measurement

Lignin content was measured by the thioglycolic acid method [29]. Ultraviolet (UV) absorbance of thioglycolic acid lignin was measured at 280 nm with a SH-1000 Lab Microplate Reader (Corona Electric Co., Ltd., Ibaraki, Japan). Lignin amount was calculated from UV absorbance using a following equation:

$$\text{Lignin concentration}\left(\text{mg L}^{-1}\right) = Abs280 \times 233.42 \quad (1)$$

where *Abs280* is a value of UV absorbance of thioglycolic acid lignin at 280 nm. The equation was obtained from a calibration curve constructed using milled wood lignins from bamboo as a standard [29].

Determination of neutral sugar composition

CWRs were de-starched [16] and the matrix polysaccharides were hydrolyzed with 2 M trifluoroacetic acid at 100 °C for 5 h. The resulting monomeric sugars were derivatized by the alditol acetate method [30] and quantified by gas chromatography mass spectrometry (GC-MS) analysis (GCMS-QP 2010 Plus, Shimadzu Co., Ltd., Kyoto, Japan). The GC-MS was operated under the following conditions: column, SUPELCO SP-2330 (30 m × 0.25 mm i.d., film thickness 0.20 μm); carrier gas, helium; oven temperature, increased from 170 °C to 235 °C at 4 °C min^{-1}; and electron ionization, 70 eV. Myo-inositol (Nacalai Tesque, Kyoto, Japan) was used as an internal standard for quantification. In parallel,

pellets left after the trifluoroacetic acid hydrolysis were treated with Updegraff reagent [31], washed with distilled water and acetone, and then completely hydrolyzed with H_2SO_4 [32]. The released glucose was quantified using a Glucose CII test kit (Wako Pure Chemicals Industries, Osaka, Japan). The amounts of polysaccharides from neutral sugar monomers were calculated as follows [33]:

$$\text{Polysaccharide content (\%)} = \textit{Monomeric sugar yield} \times C_{corr}/\textit{Dry weight}_{sample} \times 100 \quad (2)$$

where *Monomeric sugar yield*, C_{corr}, and $\textit{Dry weight}_{sample}$ are amounts (mg) of monomeric neutral sugars, correction constant: 0.90 for hexoses (glucose, mannose, and galactose); 0.88 for pentoses (xylose and arabinose), and amounts (mg) of sample used for the analysis, respectively.

Thioacidolysis

Analytical thioacidolysis was performed according to an established method [34], and the released lignin monomers were derivatized with *N*,*O*-bis(trimethylsilyl) acetamide and quantified by GC-MS (GCMS-QP 2010 Ultra, Shimadzu) using the conditions described previously [16].

2D NMR

Cell wall samples for NMR were prepared using an established method [27,35,36]. Briefly, each CWR sample (approximately 200 mg) was ground to powder in a planetary micro mill (Pulverisette 7, Fritsch Industrialist, Idar-Oberstein, Germany) in ZrO_2 vessels containing ZrO_2 ball bearings (600 rpm, eight cycles of 10 min with 5 min intervals). Then, each powdered CWR (approximately 60 mg) was swelled in 600 µL of DMSO-d_6/pyridine-d_5 (4:1, v/v) and submitted to NMR analysis. NMR spectra were acquired on an Avance III 800US system (Bruker Biospin, Billerica, MA) equipped with a cryogenically cooled 5-mm TCI gradient probe. Adiabatic 2D ^{1}H–^{13}C heteronuclear single-quantum coherence (HSQC) NMR experiments were carried out using standard implementation ("hsqcetgpsp.3") with the parameters described in the literature [36]. Data processing and analysis were conducted using Bruker TopSpin 3.1 software (Bruker Biospin, Billerica, MA), and the central DMSO solvent peaks (δ_C/δ_H = 39.5/2.49 ppm) were used as an internal reference. HSQC plot data were obtained using typical matched Gaussian apodization (line broadening = –1.0, Gaussian max. position for gm = 0.001) in F2, and squared cosine-bell apodization and one level of linear prediction (16 coefficients) in F1. Volume integrations of HSQC contours were performed as described previously [37] with a slight modification. For integration of lignin and aromatic signals, C_2–H_2 correlations from G units (**L_G**) and ferulate residues (**FA**), and C_2–H_2/C_6–H_6 correlations from S units (**L_S**), *p*-hydroxyphenyl units (**L_H**), and *p*-coumarate residues (***p*CA**), and $C_{2'}$–$H_{2'}$/$C_{6'}$–$H_{6'}$ correlations from tricin residues (**T**) were used, and the **L_S**, **L_H**, ***p*CA**, and **T** integrals were logically halved. For integrations of lignin inter-monomeric linkages, well-resolved C_α–H_α contours from β–5 (**II**), β–β (**III**), and the corresponding γ-acylated units (**II′** and **III′**), and C_β–H_β contours from β–*O*–4 units without and with γ-acylation (**I** and **I′**) were integrated, and **III** and **III′** integrals were logically halved.

Alkaline treatment

Alkaline treatment was carried out in a similar manner to that described previously [38,39]. Briefly, 60 mg of CWR was put into a 15-mL centrifuge tube, and 6 mL of 1 M NaOH (degassed by N_2) was added. The suspension was incubated at room temperature with vertical shaking at 80 rpm for 24 h in the dark. Then, the residue and supernatant were separated by centrifugation (1,000 × *g*, 10 min, room temperature). The residue was washed twice with 3 mL of methanol and dried *in vacuo*. Mass recovery rate after alkaline treatment and delignification rate by the treatment were calculated as follows:

$$\text{Mass recovery rate (\%)} = \left(CWR_U - CWR_A\right)/CWR_A \times 100 \quad (3)$$

$$\text{Delignification rate (\%)} = \left(\textit{Lignin cont.}_U \times CWR_U - \textit{Lignin cont.}_A \times CWR_A\right)/\textit{Lignin cont.}_A \times 100 \quad (4)$$

where CWR_U and CWR_A are dry weights (mg) of CWR before and after alkaline treatment, and where $\textit{Lignin cont.}_U$ and $\textit{Lignin cont.}_A$ are lignin contents (%) before and after alkaline treatment, respectively.

Determination of enzymatic saccharification efficiency

Enzymatic saccharification was performed as described previously [16]. Briefly, de-starched CWR sample (2 mg) was suspended with 200 µL of 50 mM sodium citrate buffer (pH 4.8), and 400 µL of an enzyme mixture containing 3.3 FPU Celluclast 1.5L, 7.5 CbU Novozyme 188, and 0.205 mg Ultraflo L (Novozymes, Bagsbaerd, Denmark) was added to the suspension. The reaction mixture was incubated in a rotary heat-block at 12.5 rpm and 50 °C for 24 h, and the released glucose was quantified using a Glucose CII test kit (Wako Pure Chemicals Industries). The enzymatic saccharification efficiency (ESE) was determined using the following equation:

$$\text{ESE (\%)} = Glu_E/Glu_A \times 100$$

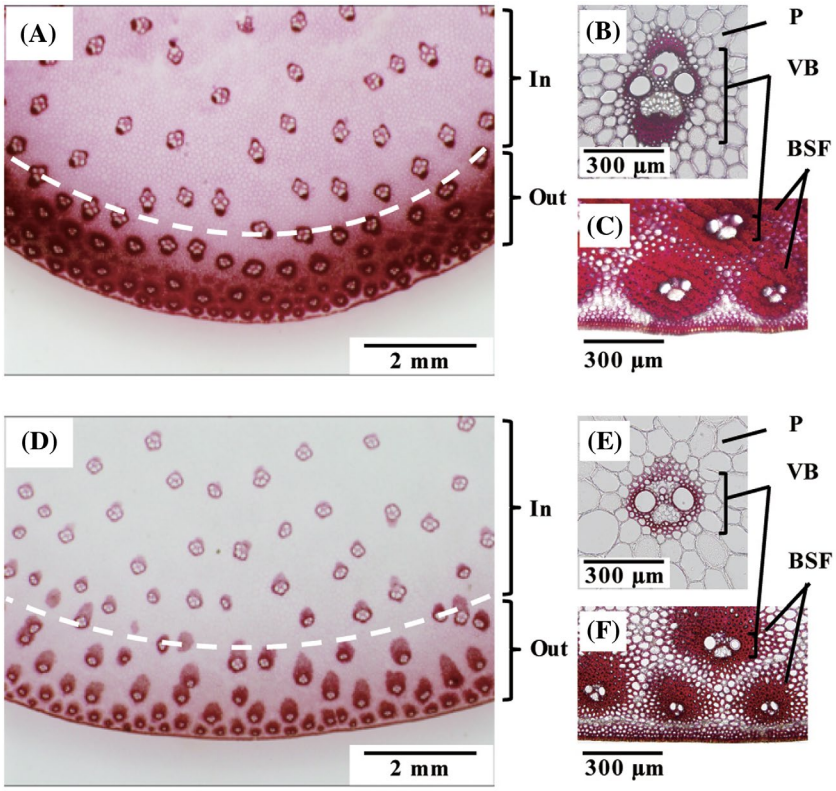

Figure 1. Histochemical analysis of internode tissues of *Erianthus* (A–C) and sugarcane (D–F). (A and D) Transverse tissue sections stained with phloroglucinol-HCl for lignin detection. Inner (In) and outer (Out) internode fractions for cell wall structure and digestibility analyses are indicated. (B and E) Magnifications of the inner internode tissues. (C and F) Magnifications of the outer internode tissues. P, parenchyma; VB, vascular bundle; BSF, bundle sheath fiber.

where Glu_E and Glu_A are the amounts (mg) of glucose obtained from the enzymatic digestion and H_2SO_4 hydrolysis [32] of CWR, respectively. The ESE improvement with alkaline treatment was evaluated using the following equation:

$$\text{ESE improvement} = ESE_U - ESE_A$$

where ESE_U and ESE_A are the ESEs determined for the untreated and alkaline-treated CWRs, respectively.

Results and discussions

Original lignocellulose structures of Erianthus *and sugarcane internode tissues*

As previously described [10,16], our histochemical analysis showed that the internode tissues of *Erianthus* and sugarcane were heterogeneously lignified. The phloroglucinol-HCl staining, which detects cinnamaldehyde end-groups in lignin polymers, indicated that vascular bundles and bundle sheath fibers were particularly lignified in both species (Figure 1). Heavily lignified vascular bundles and bundle sheath fibers were more abundant in the outer parts than the inner parts of both *Erianthus* and sugarcane internodes (Figure 1). For lignocellulose characterizations, we fractionated the inner and outer internode tissues from *Erianthus* and sugarcane.

As expected from the histochemical analysis data, both species displayed higher thioglycolic acid lignin contents in the outer internode tissues than in the inner internode tissues (Table 1). The lignin content in the inner internode tissues was 40% higher in *Erianthus* than that in sugarcane, whereas the lignin contents in the outer internode tissues were similar in the two species (Table 1). In line with this, contents of polysaccharides, i.e. arabinan, xylan, galactan, and glucan, of the inner internode tissues were higher in sugarcane than those in *Erianthus* (Table 2).

Thioacidolysis analysis was performed to determine lignin aromatic composition associated with β-*O*-4 substructures in the lignin polymers. The range for the S/G ratios of the sugarcane internode tissues was 1.4–2.2 (Table 1), and these ratios were much higher than those

Table 1. Lignin content and composition of inner and outer internode tissues of *Erianthus* and sugarcane.

		Thioglycolic acid lignin content (%)	Thioacidolysis-derived lignin composition	
			H/G[a]	S/G[a]
Erianthus	Inner	18.3 ± 0.6**	0.03 ± 0.00	0.89 ± 0.05*
	Outer	23.7 ± 0.4	0.04 ± 0.00*	0.99 ± 0.05**
Sugarcane	Inner	13.1 ± 0.8	0.05 ± 0.02	2.17 ± 0.47
	Outer	24.1 ± 0.2	0.06 ± 0.01	1.41 ± 0.18

Values are means ± standard deviations ($n = 3$). [a]GC-MS peak area ratios for lignin-derived thioacidolysis monomers:
H, *p*-hydroxyphenyl trithioethylpropane (*m/z* 239); G, guaiacyl trithioethylpropane (*m/z* 269); S, syringyl trithioethylpropane (*m/z* 299). Asterisks indicate significant differences between *Erianthus* and sugarcane in the same part of internode tissues (*$p < 0.05$; **$p < 0.01$, Student's *t*-test).

Table 2. Polysaccharide contents of inner and outer internode tissues of *Erianthus* and sugarcane.

		Polysaccharide contents (% of CWR)					
		TFA-soluble fraction					TFA-insoluble fraction
		Arabinan	Xylan	Mannan	Galactan	Glucan	Glucan
Erianthus	Inner	2.29 ± 0.10**	9.8 ± 0.7**	0.12 ± 0.05*	0.46 ± 0.13**	1.1 ± 0.3**	38.5 ± 0.9
	Outer	1.11 ± 0.03*	8.2 ± 0.1	0.12 ± 0.10	0.18 ± 0.02	0.9 ± 0.2*	46.2 ± 2.1**
Sugarcane	Inner	3.36 ± 0.06	14.4 ± 1.2	0.24 ± 0.06	1.05 ± 0.14	5.4 ± 0.7	37.6 ± 1.4
	Outer	1.93 ± 0.25	10.5 ± 1.4	0.41 ± 0.30	0.45 ± 0.18	1.8 ± 0.6	38.2 ± 0.6

Values are means ± standard deviations ($n = 3$). Asterisks indicate significant differences between *Erianthus* and sugarcane in the same internode tissues (*$p < 0.05$; **$p < 0.01$, Student's *t*-test).

in the *Erianthus* internode tissues (range 0.89–0.99). Interestingly, the differences between the S/G ratios for the outer and inner internode tissues showed opposite tendencies in *Erianthus* and sugarcane. For sugarcane, the S/G ratio was higher in the inner than that in the outer internode tissues, whereas for *Erianthus*, the ratio for the outer internode tissues was slightly higher than that for the inner internode tissues (Table 1). It has been reported that the S/G ratio in maize (*Zea mays*) internode tissues is higher in the inner part than that in the outer part [40], which is similar to what we observed for sugarcane. By contrast, in Napier grass, the S/G ratios in the internode tissues do not differ much between the inner and outer parts [41]. *p*-Hydroxyphenyl was a relatively minor component in all of the *Erianthus* and sugarcane tissues (Table 1).

For a more in-depth analysis of the lignin structures, we performed 2D HSQC-NMR analyses on the *Erianthus* and sugarcane cell wall samples (Figure 2 and Figure S2). In the aromatic sub-regions of the HSQC spectra (δ_C/δ_H 90–135/6.0–8.0 ppm), typical lignin aromatic signals from G and S units ($\mathbf{L_G}$ and $\mathbf{L_S}$), and from *p*-hydroxyphenyl ($\mathbf{L_H}$), albeit at much lower levels, were obvious. Quantitative integration data for these lignin aromatic signals (Figure 3) generally agreed with the data obtained by thioacidolysis (Table 1), indicating S/G ratios were higher in sugarcane than those in *Erianthus*. For the internode tissue fractions, the results indicated

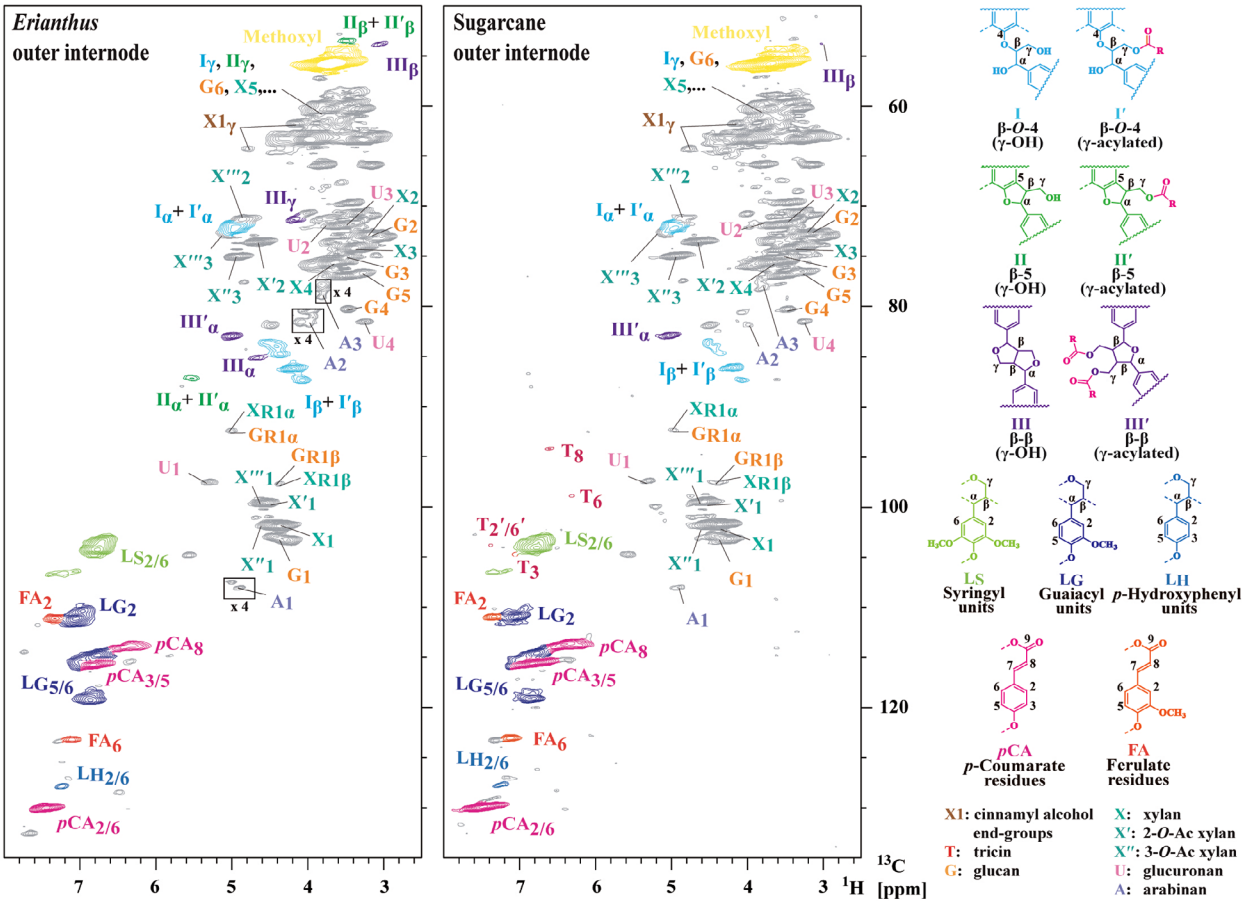

Figure 2. Two-dimensional heteronuclear single-quantum coherence nuclear magnetic resonance spectra of cell walls from outer internode tissues of *Erianthus* and sugarcane. Peak annotations are from the literature [36] and color-coded to match the structures. Boxes labeled × 4 indicate regions that are vertically scaled.

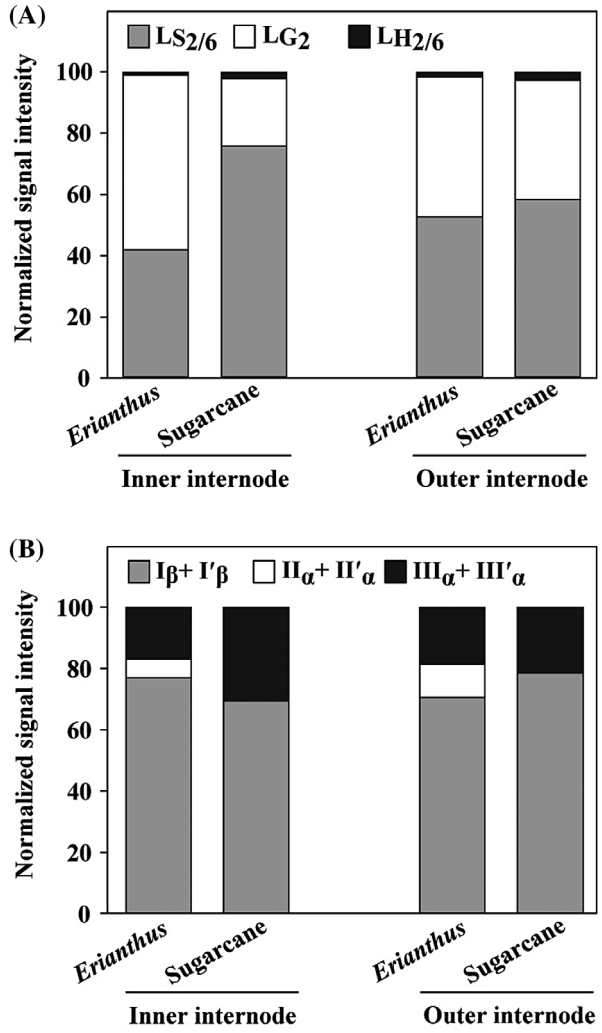

Figure 3. Normalized intensities of two-dimensional heteronuclear single-quantum coherence nuclear magnetic resonance spectroscopy signals in the spectra of the inner and outer internode cell walls from *Erianthus* and sugarcane. (A) Lignin aromatic signals expressed as a percentage of the total signal. $LS_{2/6}$, C_2–H_2/C_6–H_6 correlations from syringyl units; L_{G2}, C_2–H_2 correlations from guaiacyl units; and $LH_{2/6}$, C_2–H_2/C_6–H_6 correlations from *p*-hydroxyphenyl units. (B) Lignin inter-monomeric linkage signals expressed as a percentage of the total signal. I_β + I'_β, C_β–H_β contours from β–*O*–4 linkages; II_α + II'_α, C_α–H_α contours from β–5 linkages; and III_α + III'_α, C_α–H_α contours from β–β linkages. For structure abbreviations, see Figure 2.

that the S/G ratios were higher in the inner part than those in the outer part for sugarcane, and vice versa for *Erianthus*. In addition to the typical lignin aromatic rings, signals from *p*-coumarates and ferulates attached to lignins and/or arabinoxylans [42] were observed. Moreover, weak signals from tricin (**T**), which was recently identified as a component of lignins in grasses, were detected in the outer internode tissues of sugarcane. Interestingly, tricin signals were not detected in any of the internode tissues from *Erianthus*, suggesting much lower levels of lignin-bound tricin in *Erianthus* internodes compared to in sugarcane internodes (Figure 2). In fact, it has been reported that, although found rather ubiquitously in grass species, the levels of tricin-incorporation into lignins greatly varies with the species and organ/tissue types [44].

The aliphatic sub-regions of the HSQC spectra (δ_C/δ_H 50–90/3.0–6.0 ppm) provided information about the inter-monomeric linkages present in the lignins (Figure 2). All the spectra displayed intense signals from cell wall polysaccharides, and well-resolved prominent signals from the β–*O*–4 (**I**), β–5 (**II**), and β–β (**III**) lignin substructures as well as those from the corresponding γ-acylated substructures (**I′**, **II′**, and **III′**). The most dominant signals were from β–*O*–4 linkages (**I** and **I′**, 69–79% of the total inter-monomeric linkage signals detected) in both the *Erianthus* and sugarcane spectra (Figure 3). The β–5 linkage signals (**II** and **II′**) were detected only in the *Erianthus* spectra. S lignins lack β–5 linkages, and the absence of β–5 signals is therefore likely because of the S-rich nature of sugarcane lignins. Collectively, our analyses for original lignocellulose structure revealed differences in lignin chemical structures between *Erianthus* and sugarcane, and between parts of internode tissues from the same species.

Impact of alkaline treatment on the lignocellulose structure of Erianthus *and sugarcane internode tissues*

Next, we investigated the impact of alkaline treatment on the lignocelluloses from *Erianthus* and sugarcane tissues. Mass recovery rates after alkaline treatment were 68–76% for *Erianthus* and 62–64% for sugarcane internode tissues, and delignification rates by alkaline treatment were 41–64% for the former and 54–68% for the latter (Figure 4). The delignification rate for the outer internode tissues was significantly higher in sugarcane than that in *Erianthus*, which was in line with their difference in mass recovery rate, whereas both the mass recovery rate and delignification rate for the inner internode tissues were similar for the two species (Figure 4).

We also used 2D NMR to investigate changes in the lignocellulose structures by alkaline treatment. Our NMR data clearly showed that *p*-coumarate and ferulate units attached to lignins and/or arabinoxylans via alkali-labile ester linkages completely disappeared after the alkaline treatment of all tissues from *Erianthus* and sugarcane internodes (Figure 5, Figures S2, and S3). The tricin signals were also disappeared after the alkaline treatment of the outer internode tissues of sugarcane (Figure 5). Because lignin-bound tricin typically occurs as an end unit of a lignin polymer chain, it tends to present in lower molecular fractions of lignins [43,44]. Therefore, the notable decrease of tricin-integrated lignins might be due to the preferential solubilization of low-molecular-weight lignin fractions in alkaline treatment of sugarcane. In addition, alkaline treatment altered the

S/G composition of the residual lignins differently in the two species, and in the inner and outer internode tissues. The S signals were decreased after the alkaline treatment of the outer internode tissues of *Erianthus* and also of both the inner and outer internode tissues of sugarcane, whereas the G signals were increased after the treatment of those samples (Figure 5). The shifts in S/G composition after the alkaline treatment were corroborated by thioacidolysis (Fig. S4), and suggested that S was preferentially solubilized over G in the outer internode tissues of *Erianthus* and both the inner and outer internode tissues of sugarcane. Similar results were reported for alkaline delignification treatments of lignocellulosic samples from bamboo [25] and sorghum [26]. Our alkaline treatment was conducted with 1 M NaOH at room temperature, which is unlikely to cause cleavages of the lignin polymer backbone in general [45,46]. The preferential solubilization of S lignins by the alkaline treatment examined in this study therefore might be associated with different localization and/or molecular weight of S and G lignin polymers in the internode tissue samples of *Erianthus* and sugarcane. In contrast, however, the NMR and thioacidolysis analyses indicated that the S/G composition was increased after the alkaline treatment of the inner internode tissues of *Erianthus*. Overall, our data suggest different assemblies of lignin polymers in fractionated internode tissues from the two species: S units were likely dominant in an alkaline-soluble lignin fraction in the outer internode tissues from *Erianthus* and both inner and outer internode tissues from sugarcane; by contrast, G units would be dominant in the alkaline-soluble fraction in the inner internode tissues from *Erianthus*.

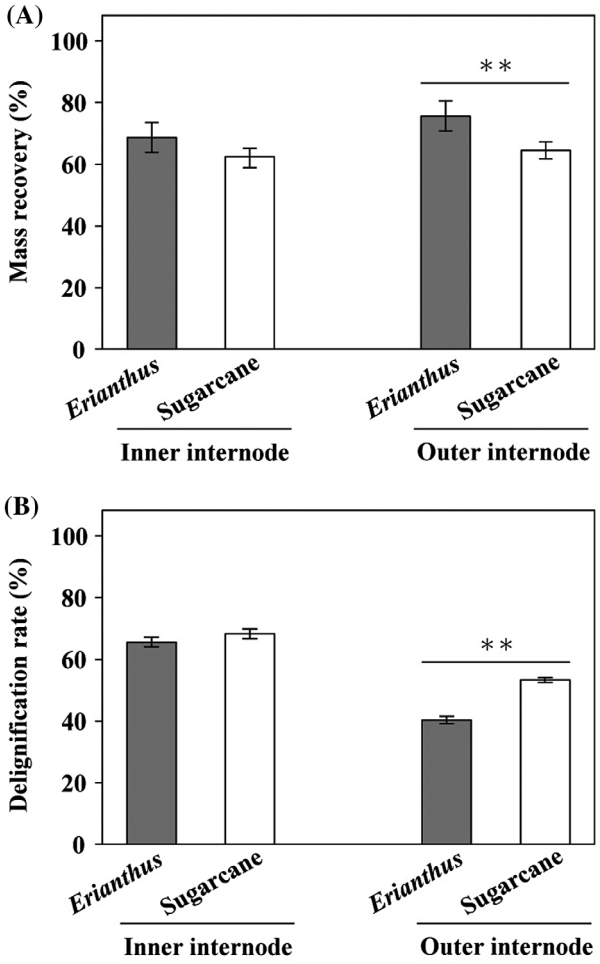

Figure 4. Mass recovery rate after alkaline treatment (A) and delignification rate by alkaline treatment (B) of inner and outer internode tissues from *Erianthus* and sugarcane. Values are means ± standard deviations (n = 3). Asterisks indicate significant differences between *Erianthus* and sugarcane tissues (**P < 0.01, Student's t-test).

In contrast to the S/G composition, the inter-monomeric linkage distributions before and after the alkaline treatment were similar for all tissues tested. The relative intensities of the β–*O*–4 linkage signals increased, whereas those of the β–β linkage signals decreased (Figure 5). The β–*O*–4 and β–β units represent the "internal" and "starting" structures in the lignin polymer chain, respectively [47]. Our data suggest that a β–β-abundant fraction of the lignin polymers was preferentially solubilized by alkaline treatment of both *Erianthus* and sugarcane internode tissues.

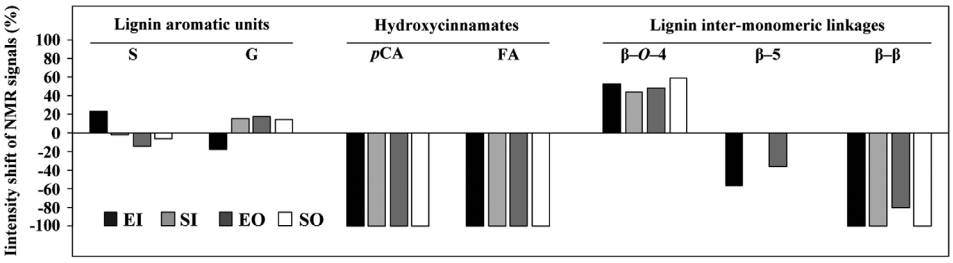

Figure 5. Changes in the lignin and *p*-hydroxycinnamate structures with alkaline treatment of inner and outer internode tissues from *Erianthus* and sugarcane as determined by two-dimensional heteronuclear single-quantum coherence (HSQC) nuclear magnetic resonance spectroscopy. HSQC signal intensities were measured for the signals from lignin aromatic units (syringyl and guaiacyl), *p*-hydroxycinnamate residues (*p*-coumarate and ferulate), and lignin inter-monomeric linkages (β–*O*–4, β–5, and β–β) both before and after the alkaline treatment. The intensity shifts with alkaline treatment were calculated. For structure abbreviations, see Figure 2. EI and EO, the inner and outer internode tissues from *Erianthus*, respectively. SI and SO, the inner and outer internode tissues from sugarcane, respectively.

Table 3. Enzymatic saccharification efficiencies (ESEs) and summary of lignocellulose characteristics of untreated and alkaline-treated *Erianthus* and sugarcane internode tissues.

		Untreated			Alkali-treated			ESE improvement (%)
		ESE (%)	Lignin content (%)	Lignin S/G ratio	ESE (%)	Lignin content (%)	Lignin S/G ratio	
Erianthus	In	13.7 ± 0.3A	18.3 ± 0.6A	0.89 ± 0.05A	82.8 ± 3.0a	9.2 ± 0.4a	0.99 ± 0.02a	69.0 ± 3.0a
	Out	7.3 ± 0.4B	23.7 ± 0.4B	0.99 ± 0.05A	54.3 ± 1.3b	18.7 ± 0.4b	0.94 ± 0.10a	47.0 ± 1.3b
Sugarcane	In	55.2 ± 4.3C	13.1 ± 0.8C	2.17 ± 0.47AB	94.0 ± 1.9c	6.7 ± 0.3c	1.57 ± 0.20b	38.9 ± 1.9c
	Out	24.3 ± 1.5D	24.1 ± 0.2B	1.41 ± 0.18B	85.8 ± 4.3a	17.5 ± 0.3d	1.14 ± 0.05c	61.5 ± 4.3ac

Values of ESE, lignin content, lignin S/G ratio, and ESE improvement are means ± standard deviations ($n = 3$). Differences in means within a group with unlike letters are statistically significant ($p < 0.05$, Holm-adjusted t-test).

Enzymatic digestibility of Erianthus *and sugarcane internode tissues before and after alkaline treatment*

Lastly, we compared enzymatic saccharification of untreated and alkaline-treated *Erianthus* and sugarcane tissues. Enzymatic saccharification efficiencies (ESEs) of the untreated sugarcane tissues were significantly higher than those of the *Erianthus* tissues (Table 3). The inner internode tissues displayed substantially lower lignin levels in sugarcane compared with *Erianthus*, explaining the difference in ESEs of the inner internode tissues from the two species. However, interestingly, even though the lignin contents in the outer internode tissues were similar between the two species, sugarcane still displayed a substantially higher ESE than *Erianthus* (Table 3). In earlier studies, the relationship between lignin aromatic composition and lignocellulose digestibility was investigated for dehydrogenation of polymer–cell wall complexes [48], transgenic alfalfa [49], *Arabidopsis* [50], and hybrid *Saccharum* spp. [11], and the results suggested that it was unlikely that enzymatic digestibility of biomass was correlated with its lignin S/G ratio. Therefore, a relationship between digestibility and some other factors of lignocellulose besides the lignin content and S/G composition, such as the substructure distribution and supramolecular structure of lignins, should be analyzed in the future.

The ESEs of *Erianthus* and sugarcane internode tissues were greatly improved by the alkaline treatment. However, the ESEs of alkaline-treated internode tissues from *Erianthus* (54–83%) were still lower than those of sugarcane (86–94%) (Table 3). The ESE improvement by alkaline treatment in the inner internode tissues was higher in *Erianthus* than that in sugarcane, which is because the ESE of alkaline-treated inner internode from sugarcane almost reached saturation (94%). On the other hand, the ESE improvement in the outer internode tissues was significantly higher in sugarcane than that in *Erianthus*, which was correlated with their difference in alkaline delignification rate (Figure 4). Therefore, in addition to the poor digestibility of untreated biomass from *Erianthus*, the resistance of the outer internode tissues to alkaline treatment also limited the ESE of the alkaline-treated *Erianthus* biomass.

Conclusions

We demonstrated that original lignocellulose structures in *Erianthus* and sugarcane internode tissues were substantially different, not only between the two species, but also between inner and outer parts of internode tissues from the same species. In particular, our analyses indicated that G units and β–5 linkage structures in lignin polymers were more abundant in *Erianthus* tissues than those in sugarcane tissues. We observed that G units were more resistant to alkaline treatment compared with S units in the outer internode tissues from both species, which could explain a recalcitrance of the outer internode tissues from *Erianthus* to alkaline delignification. Enzymatic saccharification efficiencies for the alkaline-treated samples were still higher in sugarcane than those in *Erianthus*. Taken together, our data suggest that different assemblies of lignin polymers in *Erianthus* and sugarcane affected alkaline delignification efficiency and enzymatic saccharification efficiency of their biomass. In addition, we also observed other differences in lignocelluloses from *Erianthus* and sugarcane, such as tricin level, whose impacts on biomass properties will deserve further analysis.

Author contributions

T. M., M. Y., K. T., Y. Te., Y. K., and T. U. conceived and designed the research. T. M., M. Y., Y. To., S. S., M. K., A. M. performed experiments and analyzed data. T. M. and T. U. wrote the manuscript with supports from all the other authors.

Acknowledgements

We thank Kamigamo Experimental Station, Field Science Education and Research Center, Kyoto University, Japan, for providing *E. arundinaceus* plants. We also thank Ms. Naoko Tsue and Ms. Keiko Tsuchida for their assistance in chemical analysis, and Dr. Hironori Kaji and Ms. Ayaka Maeno for their assistance in NMR analysis. A part of this study was conducted using the facilities in the Development and Assessment of Sustainable Humanosphere/Forest Biomass Analytical System at the Research Institute for Sustainable Humanosphere, Kyoto University, and using the NMR spectrometer in the Joint Usage/Research Center at the Institute for Chemical Research, Kyoto University.

Disclosure statement

The authors have no competing financial interests to declare.

Funding

This work was supported by the New Energy and Industrial Technology Development Organization through the project "Development of Efficient Element Technology for Biofuel Production,"; the Japan Science and Technology Agency/ Japan International Cooperation Agency through the project "Science and Technology Research Partnership for Sustainable Development"; and the Research Institute for Sustainable Humanosphere, Kyoto University [grant number [2016-5-2-1].

ORCID

Toshiaki Umezawa http://orcid.org/0000-0003-1135-5387

References

[1] Pauly M, Keegstra K. Cell-wall carbohydrates and their modification as a resource for biofuels. Plant J. 2008;54(4):559–568.
[2] Hattori T, Morita S. Energy crops for sustainable bioethanol production; which, where and how? Plant Prod. Sci. 2010;13(3):221–234.
[3] Ra K, Shiotsu F, Abe J, et al. Biomass yield and nitrogen use efficiency of cellulosic energy crops for ethanol production. Biomass Bioenerg. 2012;37(5):330–334.
[4] Mislevy P, Martin FG, Adjei MB, et al. Harvest management effects on quantity and quality of *Erianthus* plant morphological components. Biomass Bioenerg. 1997;13(1–2):51–58.
[5] Augustine SM, Syamaladevi DP, Premachandran MN, et al. Physiological and molecular insights to drought responsiveness in *Erianthus* spp. Sugar Tech. 2015;17(2):121–129.
[6] Matsuo K, Chuenpreecha T, Matsumoto N, et al Eco-physiological characteristics of *Erianthus* spp. and yielding abilities of three forages under conditions of cattle feces application. JIRCAS Working Rep. 2002;30:187–194.
[7] Matsunami H, Kobayashi M, Ando S, et al. Turnover of minerals and nonstructural carbohydrates in *Erianthus arundinaceus* (L.) Beauv. during winter in temperate Japan. Jpn J Grassl Sci. 2014;59(4):246–252. (in Japanese with English Summary).
[8] Matsunami H, Kobayashi M, Ando S, et al. Sources of nitrogen taken up by *Erianthus arundinaceus* (L.) Beauv. Jpn J Grassl Sci. 2014;60(2):97–101. (in Japanese with English Summary).
[9] Aitken K, Li J, Wang L, et al. Characterization of intergeneric hybrids of *Erianthus rockii* and *Saccharum* using molecular markers. Genet Resour Crop Evol. 2007;54(7):1395–1405.
[10] Bottcher A, Cesarino I, Santos AB, et al. Lignification in sugarcane: biochemical characterization, gene discovery, and expression analysis in two genotypes contrasting for lignin content. Plant Physiol. 2013;163(4):1539–1557.
[11] Chong BF, Bonnett GD, O'Shea MG. Altering the relative abundance of hydroxycinnamic acids enhances the cell wall digestibility of high-lignin sugarcane. Biomass Bioenerg. 2016;91:278–287.
[12] Sun JX, Sun XF, Sun RC, et al. Inhomogeneities in the chemical structure of sugarcane bagasse lignin. J Agric Food Chem. 2003;51(23):6719–6725.
[13] Li Y, Qi B, Luo J, et al. Effect of alkali lignins with different molecular weights from alkali pretreated rice straw hydrolyzate on enzymatic hydrolysis. Bioresour Technol. 2016;200:272–278.
[14] Nakagame S, Chandra RP, Kadla JF, et al. Enhancing the enzymatic hydrolysis of lignocellulosic biomass by increasing the carboxylic acid content of the associated lignin. Biotechnol Bioeng. 2011;108(3):538–548.
[15] Horikawa Y, Imai T, Takada R, et al. Chemometric analysis with near-infrared spectroscopy for chemically pretreated erianthus toward efficient bioethanol production. Appl Biochem Biotechnol. 2012;166(3):711–721.
[16] Yamamura M, Noda S, Hattori T, et al. Characterization of lignocellulose of *Erianthus arundinaceus* in relation to enzymatic saccharification efficiency. Plant Biotechnol. 2013;30(1):25–35.
[17] Studer MH, DeMartini JD, Davis MF, et al. Lignin content in natural *Populus* variants affects sugar release. Proc Natl Acad Sci USA. 2011;108(15):6300–6305.
[18] Murashima K, Kosugi A, Doi RH. Synergistic effects of cellulosomal xylanase and cellulases from clostridium cellulovorans on plant cell wall degradation. J Bacteriol. 2003;185(5):1518–1524.
[19] Wang L, Zhang Y, Gao P, et al. Changes in the structural properties and rate of hydrolysis of cotton fibers during extended enzymatic hydrolysis. Biotechnol Bioeng. 2006;93(3):443–456.
[20] Kumari S, Das D. Improvement of gaseous energy recovery from sugarcane bagasse by dark fermentation followed by biomethanation process. Bioresour Technol. 2015;194:354–363.
[21] Mclntosh S, Vancov T. Enhanced enzyme saccharification of *Sorghum bicolor* straw using dilute alkali pretreatment. Bioresour Technol. 2010;101(17):6718–6727.
[22] Phitsuwan P, Sakka K, Ratanakhanokchai K. Structural changes and enzymatic response of Napier grass (*Pennisetum purpureum*) stem induced by alkaline pretreatment. Bioresour Technol. 2016;218:247–256.
[23] Pu Y, Zhang D, Singh PM, et al. The new forestry biofuels sector. Biofuels Bioprod Bioref. 2008;2(1):58–73.
[24] Xu N, Zhang W, Ren S, et al. Hemicelluloses negatively affect lignocellulose crystallinity for high biomass digestibility under NaOH and H_2SO_4 pretreatments in *Miscanthus*. Biotechnol Biofuels. 2012;5:58.
[25] Wen JL, Sun SL, Xue BL, et al. Structural elucidation of inhomogeneous lignins from bamboo. Int J Biol Macromol. 2015;77:250–259.
[26] Sun SL, Wen JL, Ma MG, et al. Revealing the structural inhomogeneity of lignins from sweet sorghum stem by successive alkali extractions. J Agric Food Chem. 2013;61(18):4226–4235.
[27] Takeda Y, Koshiba T, Tobimatsu Y, et al. Regulation of *CONIFERALDEHYDE5-HYDROXYLASE* expression to modulate cell wall lignin structure in rice. Planta. 2017;246(2):337–349.
[28] Tagane S, Ponragdee W, Sansayawichai T, et al. Characterization and taxonomical note about Thai *Erianthus* germplasm collection: the morphology, flowering phenology and biogeography among *E. procerus* and three types of *E. arundinaceus*. Genet Resour Crop Evol. 2012;59(5):769–781.

[29] Suzuki S, Suzuki Y, Yamamoto N, et al. High-throughput determination of thioglycolic acid lignin from rice. Plant Biotechnol. 2009;26(3):337–340.
[30] Hayashi T. Measuring β-glucan deposition in plant cell walls. In: Linskens HF, Jackson JF, editors. Plant Fibers. Berlin: Springer-Verlag; 1989. p. 138–160.
[31] Updegraff DM. Semimicro determination of cellulose in biological materials. Anal Biochem. 1969;32(3):420–424.
[32] Hattori T, Murakami S, Mukai M, et al. Rapid analysis of transgenic rice straw using near-infrared spectroscopy. Plant Biotechnol. 2012;29(4):359–366.
[33] Sluiter A, Hames B, Ruiz R, et al. Determination of structural carbohydrates and lignin in biomass: laboratory analytical procedure (LAP): Issue Date, April 2008, Revision Date: August 2012 (Version 08-03-2012). National Renewable Energy Laboratory, Golden, Colorado, USA; 2012.
[34] Yamamura M, Hattori T, Suzuki S, et al. Microscale thioacidolysis method for the rapid analysis of β–*O*–4 substructures in lignin. Plant Biotechnol. 2012;29(4):419–423.
[35] Koshiba T, Yamamoto N, Tobimatsu Y, et al. MYB-mediated upregulation of lignin biosynthesis in *Oryza sativa* towards biomass refinery. Plant Biotechnol. 2017;34(1):7–15.
[36] Mansfield SD, Kim H, Lu F, et al. Whole plant cell wall characterization using solution-state 2D NMR. Nat Protoc. 2012;7(9):1579–1589.
[37] Tobimatsu Y, Chen F, Nakashima J, et al. Coexistence but independent biosynthesis of catechyl and guaiacyl/syringyl lignin polymers in seed coats. Plant Cell. 2013;25(7):2587–2600.
[38] Akin DE. Grass lignocellulose. Appl Biochem Biotechnol. 2007;137–140(1–12):3–15.
[39] Yamamura M, Wada S, Sakakibara N, et al. Occurrence of guaiacyl/*p*-hydroxyphenyl lignin in *Arabidopsis thaliana* T87 cells. Plant Biotechnol. 2011;28(1):1–8.
[40] Barros-Rios J, Santiago R, Malvar RA, et al. Chemical composition and cell wall polysaccharide degradability of pith and rind tissues from mature maize internodes. Anim Feed Sci Technol. 2012;172(3–4):226–236.
[41] del Río JC, Prinsen P, Rencoret J, et al. Structural characterization of the lignin in the cortex and pith of elephant grass (*Pennisetum purpureum*) stems. J Agric Food Chem. 2012;60(14):3619–3634.
[42] Ralph J. Hydroxycinnamates in lignification. Phytochem Rev. 2010;9(1):65–83.
[43] Lan W, Lu F, Regner M, et al. Tricin, a flavonoid monomer in monocot lignification. Plant Phyisiol. 2015;167(4):1284–1295.
[44] Lan W, Rencoret J, Lu F, et al. Tricin-lignins: occurrence and quantitation of tricin in relation to phylogeny. Plant J. 2016;88(6):1046–1057.
[45] Gierer J. Chemistry of delignification. Wood Sci Technol. 1985;19(4):289–312.
[46] Imai A, Yokoyama T, Matsumoto Y, et al. Significant lability of guaiacylglycerol β-phenacyl ether under alkaline conditions. J Agric Food Chem. 2007;55(22):9043–9046.
[47] Ralph J, Lundquist K, Brunow G, et al. Lignins: natural polymers from oxidative coupling of 4-hydroxyphenyl-propanoids. Phytochem Rev. 2004;3(1–2):29–60.
[48] Grabber JH, Ralph J, Hatfield RD, et al. p -hydroxyphenyl, guaiacyl, and syringyl lignins have similar inhibitory effects on wall degradability. J Agric Food Chem. 1997;45(7):2530–2532.
[49] Chen F, Dixon RA. Lignin modification improves fermentable sugar yields for biofuel production. Nat Biotechnol. 2007;25(7):759–761.
[50] Shi J, Pattathil S, Parthasarathi R, et al. Impact of engineered lignin composition on biomass recalcitrance and ionic liquid pretreatment efficiency. Green Chem. 2016;18(18):4884–4895.